Macromolecules
ARTICLE

Macromolecules **2009**, *42*, 4977–4984 **4977**
DOI: 10.1021/ma900598c

Synthesis of 4,7-Diphenyl-2,1,3-Benzothiadiazole-Based Copolymers and Their Photovoltaic Applications

Shanpeng Wen, Jianing Pei, Yinhua Zhou, Pengfei Li, Lili Xue, Yaowen Li, Bin Xu, and Wenjing Tian*

State Key Laboratory of Supramolecular Structure and Materials, Jilin University, Changchun 130012, P. R. China

Received March 19, 2009; Revised Manuscript Received June 1, 2009

ABSTRACT: Three novel conjugated copolymers containing alkoxylated 4,7-diphenyl-2,1,3-benzothiadiazole and dialkylfluorene or dialkyloxyphenylene or dialkylthiophene units were prepared by Horner polycondensation reactions. They are all soluble in common organic solvents such as chloroform, tetrahydrofuran, and chlorobenzene. The novel copolymers were characterized by NMR, GPC, and elemental analysis. Thermogravimetric analysis of the copolymers showed they have good thermal stability with the decomposition temperature higher than 350 °C. Cyclic voltammetric study shows that the HOMO energy levels of the three copolymers are deep-lying which implies that these copolymers have good stability in the air and the relatively low HOMO energy level assures a higher open circuit potential when they are used in photovoltaic cells. Bulk-heterojunction photovoltaic cells were fabricated with the copolymers as the donors and PCBM as the acceptor. The cells based on the three copolymers exhibited power conversion efficiencies of 0.65, 1.25, 1.62% with high open circuit potential of 0.76, 0.96, and 1.04 V under one sun of AM 1.5 solar simulator illumination (100 mW/cm^2).

1. Introduction

In recent years, considerable efforts have been directed toward the development of polymer photovoltaic cells.[1−6] The most widely used configuration of polymer photovoltaic cells is the so-called "bulk heterojunction" devices in which the active layer consists of a blend of an electron-donating conjugated polymer, and an electron-acceptor such as (6,6)-phenyl C_{61}-butyric acid methyl ester (PCBM).[7−10] Recently, such polymer cells with power conversion efficiency (PCE) as high as 5% have been realized by using a blend of regioregular poly(3-hexylthiophene) (P3HT) and PCBM as the active layer.[9,11] Further improvement on PCE entails new conjugated polymers with broader and longer wavelength absorption of the solar spectrum. However, the polymer cells using longer wavelength absorption (low band gap) polymer as donors usually exhibit low open-circuit voltages (V_{oc}), which results in low PCE.[12,13] The V_{oc} of polymer photovoltaic cells is determined by the difference between of the lowest unoccupied molecular orbital (LUMO) of acceptor and the highest occupied molecular orbital (HOMO) of donor.[14−16] Since we usually use PCBM as the acceptor, the HOMO energy level is an important parameter to be considered when designing a new electro-donating polymer.

4,7-Diphenyl-2,1,3-benzothiadiazole (DBT) and its derivatives are known to be strongly fluorescent dyes,[19] which exhibit low-lying HOMO energy level and less easy oxidization. Because of their unique electro-optical properties, polymers and small molecules containing DBT were used in various applications such as light-emitting diodes,[17] liquid crystal displays,[18] and two photon absorption.[19] On the other hand, the band gap of DBT is relatively large (2.8 eV)[20] and its absorption locates mainly in the violet or ultraviolet (UV) area—only a small proportion of sunlight, which limits its application for photovoltaic cells. However, the copolymerization of DBT with fluorene, thiophene, or other suitable aromatic units can probably afford copolymers with new electron configurations and new optoelectronic properties. In addition, the introduction of the vinylene linkage in π-conjugated systems has been an effective strategy for modulating their electronic properties.[21]

In this paper, we report the synthesis and photovoltaic properties of three new 4,7-diphenyl-2,1,3-benzothiadiazole-based copolymers: poly(fluorenevinylene-*alt*-4,7-diphenyl-2,1,3-benzothiadiazole) (PF-DBT), poly(phenylenevinylene-*alt*-4,7-diphenyl-2,1,3-benzothiadiazole) (PP-DBT), and poly(thiophenevinylene-*alt*-4,7-diphenyl-2,1,3-benzothiadiazole) (PT-DBT) by Horner polycondensation which is fit for the synthesis of well-defined strictly alternating copolymers. The optical and electrochemical properties of the three copolymers are systematically described. Photovoltaic cells based on the three copolymers with a structure of ITO/PEDOT/copolymer:PCBM/LiF/Al exhibit PCEs of 0.65, 1.25 and 1.62% under one sun of AM 1.5 solar simulator illumination (100 mW/cm^2). It should be noted that high V_{oc}s of 0.76, 0.96, and 1.04 V have been achieved from these cells due to the deep-lying HOMO energy levels of the copolymers.

2. Results and Discussion

2.1. Synthesis and Characterization. Synthetic routes of the monomers and polymers are shown in Schemes 1 and 2. Monomer (**M-1**) was synthesized in a multistep synthesis. Starting from commercially available hydroquinone, in four steps, 4-formyl-2,5-bis(hexyloxy)phenylboronic acid (**6**) was obtained. Similarly, 4,7-dibromo-2,1,3-benzothiadiazole was synthesized by a modified procedure in high yield. By Suzuki coupling of **5** with 4,7-dibromo-2,1,3-benzothiadiazole, final product (**M-1**) was obtained in good yield. The phosphonate esters (**M-2**−**M-4**) were synthesized by Michaelis−Arbuzov reaction.[22] The purity of the monomers and the intermediate compounds were confirmed by ^{1}H NMR and elemental analysis. Monomer (**M-1**) was copolymerized with monomers (**M-2**−**M-4**) by using the t-BuOK Horner coupling method.[23] The yields of the resulting polymers were over 60%. All the polymers exhibited excellent solubility in common organic

*Corresponding author. E-mail address: wjtian@jlu.edu.cn.

Published on Web 07/02/2009

Scheme 1. Syntheses of Monomers M-1-M-4[a]

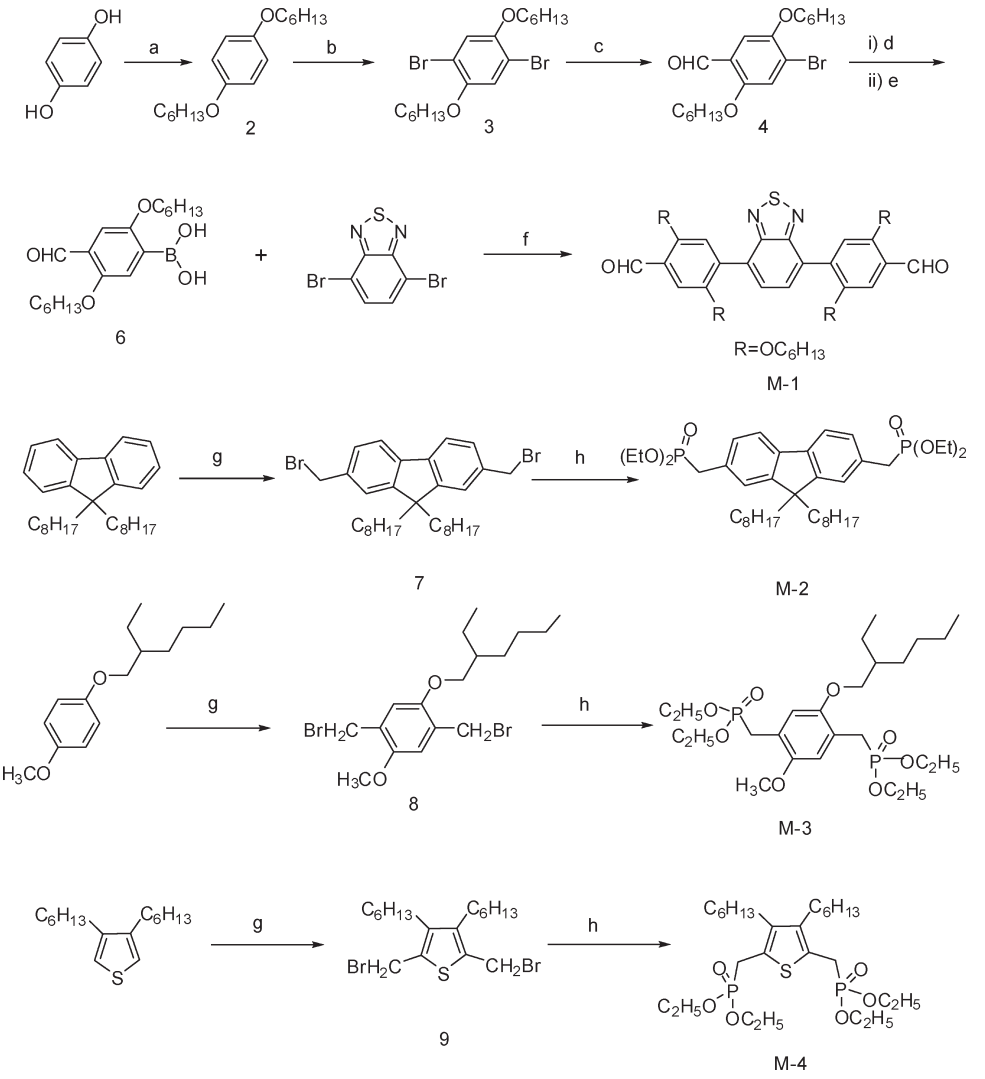

[a] Reagents and conditions: (a) 1-bromohexane, DMSO, KOH, room temperature; (b) CCl_4, bromine, room temperature; (c) THF, BuLi, DMF, −78 °C to room temperature; (d) toluene, 1,3-propandiol, $BF_3 \cdot OEt_2$, 8 h reflux; (e) (i) THF, BuLi, trimethylborate, −78 °C to room temperature, 24 h, (ii) 2 M HCl, room temperature, 20 h; (f) toluene, THF, aqueous K_2CO_3 (2 M), $Pd(PPh_3)_4$, 85 °C, 36 h; (g) formaldehyde, aqueous HBr, glacial CH_3COOH, room temperature, 24 h; (h) triethylphosphite, 150 °C, 24 h.

Scheme 2. Syntheses of Copolymers

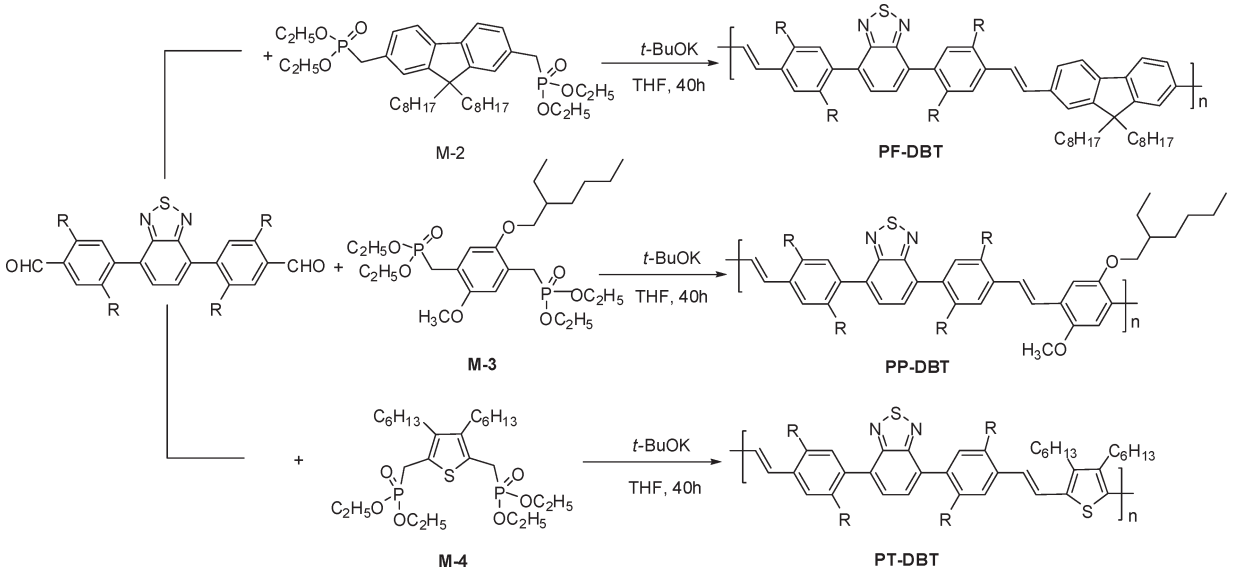

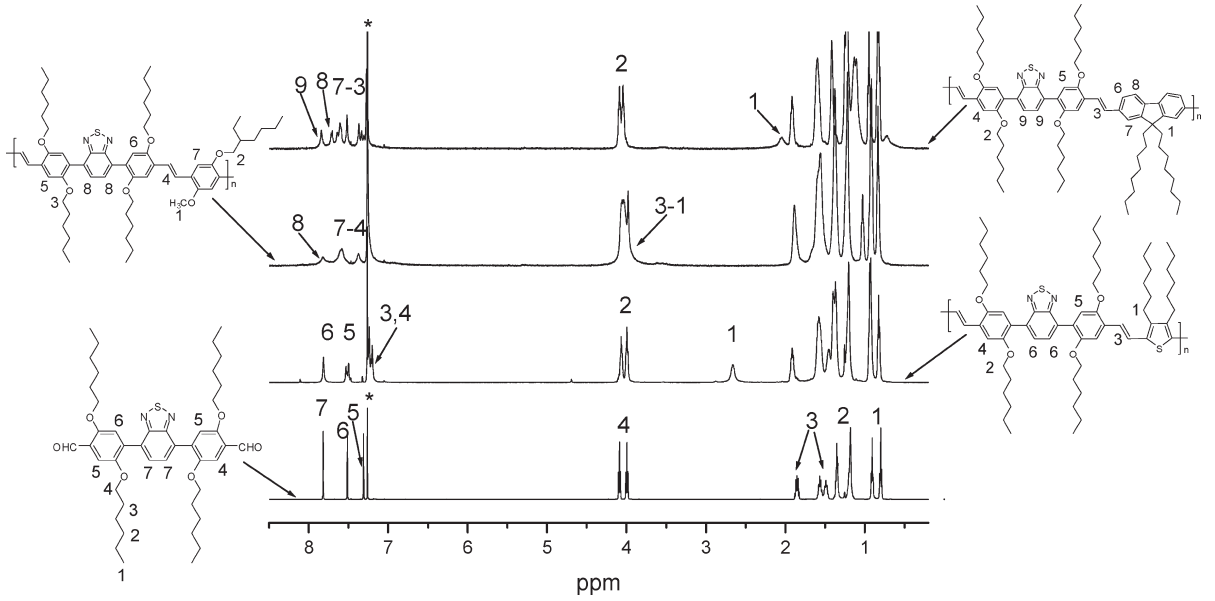

Figure 1. 500 MHz-^{1}H NMR spectra of monomer M-1 and copolymers PF-DBT, PP-DBT, and PT-DBT.

Table 1. Polymerization Results and Thermal Properties of Copolymers

polymer	yield (%)	M_n (10^4)	M_w (10^4)	PDI	TGA (T_d)
PF-DBT	65	2.9	6.30	2.17	389
PP-DBT	70	6.2	12.2	1.95	358
PT-DBT	68	2.1	5.10	2.41	380

solvents such as chloroform, tetrahydrofuran, and chlorobenzene. The ^{1}H NMR spectra of monomer (**M-1**) and the three copolymers are shown in Figure 1. All spectra show signals of the DBT phenylene protons at about 7.31, 7.51, and 7.81 ppm, and signals of hexyloxy-substituted chains of DBT in the region from 0.7 to 1.9 ppm. The signal of the methylene group adjacent to O atom of the DBT unit appears at around 4.0 ppm.[24] For the fluorene-containing copolymer **PF-DBT**, the signal of the methylene group adjacent to the fluorene C_9 atom appears at 2.04 ppm.[25] The signals of the fluorene ring occur at 7.71 and 7.61 ppm. For the dialkoxyphenylene-based copolymer **PP-DBT**, the Ar-OCH_2 protons in the 2-ethylhexyl and Ar−OCH_3 protons are merged with Ar-OCH_2 protons in DBT, while the Ar−H protons in dialkoxyphenylene are merged with Ar−H protons in DBT. For **PT-DBT**, the characteristic signal of the α methylene group linked to the thiophene occurs at 2.66 ppm.[23]

The molecular weights and polydispersities of the resulting polymers were determined by gel permeation chromatography (GPC) analysis with a polystyrene standard calibration with the number average molecular weight (M_n) of 21 000−62 000, weight average molecular weight (M_w) of 51 000−122 000, and PDI (poly dispersity index, M_w/M_n) of 1.95−2.41. Table 1 summarizes the polymerization results including molecular weights, PDI and thermal stability of the polymers.

2.2. Thermal Properties. Figure 2 shows the thermogravimetric analysis (TGA) curves of the synthesized copolymers at the heating rate of 10 °C/min under a nitrogen atmosphere. As shown in Figure 2, the decomposition temperatures (T_d) of the copolymers are in the range of 358−389 °C, which suggests relatively high thermal stability. The high thermal stability of the resulting polymers prevents the deformation of the copolymer morphology and the degradation of the polymeric active layer under applied electric fields. The T_d of the copolymers is also summarized in Table 1.

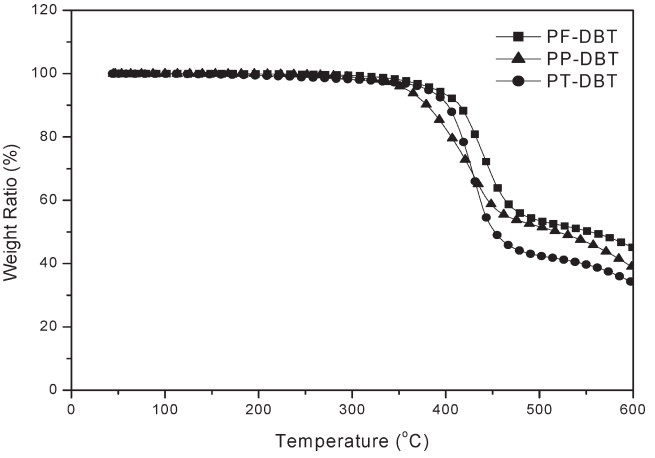

Figure 2. TGA curves of copolymers at the heating rate of 10 °C/min under nitrogen atmosphere.

2.3. Optical Properties. The UV−vis absorption spectra of the three copolymers in dilute chloroform solution (concentration 1×10^{-5} M) are shown in Figure 3a, and the maximum absorptions are listed in Table 1. For PF-DBT, two obvious optical absorption peaks located around 400 and 436 nm are attributed to the $\pi-\pi^*$ transitions of the conjugated backbone.[25] In comparison to PF-DBT, the maximum absorption peaks for PP-DBT and PT-DBT were located at 462 and 485 nm, which is 26 and 49 nm red-shifted compared to that of PF-DBT because dialkyloxyphenylene and dialkylthiophene units can provide more conjugation than dialkylfluorene unit in the conjugated backbone of the copolymers.

The optical absorption spectra of the copolymers in thin films (shown in Figure 3b) are generally similar in shape to that in dilute solution. Compared to their counterparts in dilute solution, the optical absorption of the polymers in film exhibited red shift by ca. 12−20 nm, presumably indicating the formation of a π-stacked structure in the solid state.[26,27] From the low energetic edge of the absorption spectrum of the individual copolymer, the band gap of PF-DBT was estimated to be 2.32 eV (absorption edge: ~534 nm), while smaller band gaps of 2.24 and 2.02 eV were calculated for PP-DBT and PT-DBT (absorption edges: ~554 and ~613 nm), respec-

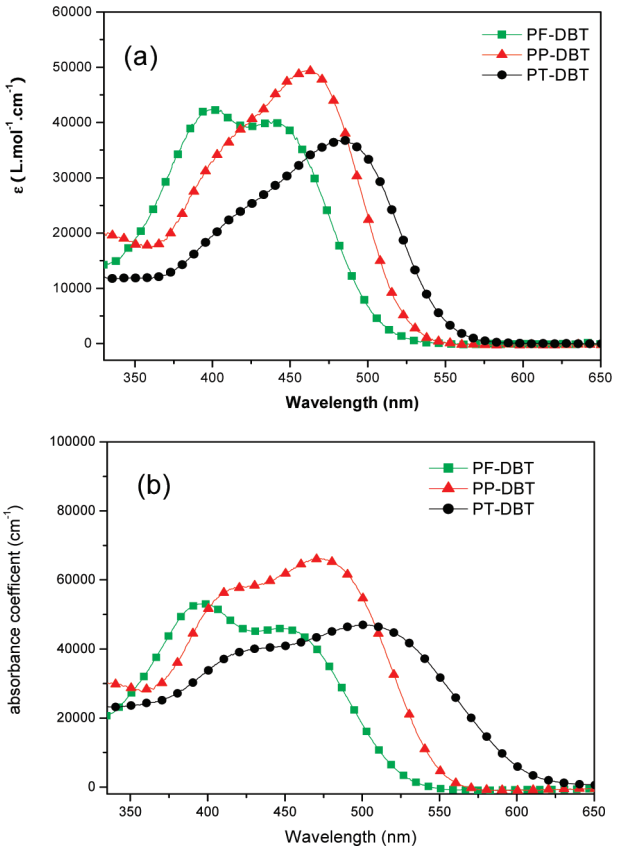

Figure 3. UV−vis absorption spectra of PF-DBT, PP-DBT, and PT-DBT in chloroform solution and (b) in thin films.

tively. The decrease of the band gap from PF-DBT to PP-DBT and PT-DBT can be explained by the greater conjugation of dialkyloxyphenylene and dialkylthiophene units than the dialkylfluorene unit in the copolymer backbones.

2.4. Electrochemical Properties. Cyclic voltammetry of the copolymer films was performed in acetonitrile with 0.1 M tetrabutylammonium hexafluorophosphate ($TBAPF_6$) as the supporting electrolyte at scan rates of 30−50 mV/s. Platinum wire electrodes were used as both counter and working electrodes, and silver/silver ion (Ag in 0.1 M $AgNO_3$ solution, from Bioanalytical Systems, Inc.) was used as a reference electrode. Ferrocene /ferrocenium (Fc/Fc^+) was used as the internal standard.

The redox curves of the copolymers are shown in Figure 4. On the anodic sweep, all copolymers showed an irreversible oxidation with an onset potentials of 0.71 V (versus Ag/Ag^+) for PF-DBT, 0.50 V for PP-DBT, and 0.38 V for PT-DBT, respectively. In contrast, the cathodic sweep showed an onset reduction potentials of −1.65 V (versus Ag/Ag^+) for PF-DBT, −1.73 V for PP-DBT, and −1.71 V for PT-DBT.

From the onset oxidation potentials (E_{ox}^{onset}) and the onset reduction potentials (E_{red}^{onset}) of the polymers, HOMO and LUMO energy levels as well as the energy gap were calculated according to the following equations:[15,28]

$$\text{HOMO (eV)} = -e(E_{ox}^{onset} + 4.73)$$

$$\text{LUMO (eV)} = -e(E_{red}^{onset} + 4.73)$$

$$E_g^{ec}\ \text{(eV)} = e(E_{ox}^{onset} - E_{red}^{onset})$$

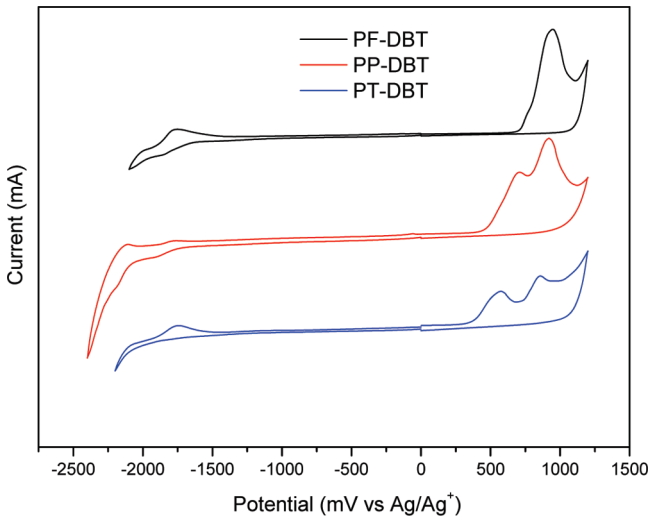

Figure 4. Cyclic voltammograms of copolymer thin films on Pt wires in 0.1 M $TBAPF_6$ in acetonitrile. The scan rates used were 30−50 mV/s.

where E_{ox}^{onset}, and E_{red}^{onset} are the measured onset potentials relative to Ag/Ag^+.

The results of the electrochemical measurements and calculated energy levels of the copolymers are listed in Table 2. From Table 2 we can see that the oxidation potential of PT-DBT is higher than that of regioregular polythiophenes, which indicates that the oxidative stability of PT-DBT is higher than that of regioregular polythiophenes.[28] The HOMO energy level of the donor polymers in a heterojunction photovoltaic cell is very important for high device efficiency, because the V_{oc} of PVC is determined by the difference between the HOMO level of the donor polymer and the LUMO of the acceptor. The relatively low HOMO level (−5.11 to −5.45 eV) of the synthesized copolymers compared with polythiophene derivatives, for example P3HT (HOMO = −4.75 eV),[28,29] may be favored for the improvement of the V_{oc} when fabricating the PVC with one of these polymers as donor and PCBM as acceptor.

2.5. Photovoltaic Properties. PVCs were fabricated with the structure of ITO/ PEDOT/PSS/active layer /LiF/Al, where the active layer consists of copolymer: PCBM (1:4, w/w). Figure 5 shows the current−voltage ($J-V$) curves of the PVCs based on the three copolymers (PF-DBT, PP-DBT, and PT-DBT): PCBM under one sun of AM 1.5 solar simulator illumination (100 mW/cm^2) and their photovoltaic parameters are summarized in Table 3. The V_{oc}, short-circuit current (J_{sc}), fill factor (FF), and PCE were measured to be 1.04 V, 2.80 mA cm^{-2}, 0.43, and 1.25% for the photovoltaic cell based on PF-DBT:PCBM; 0.96 V, 3.93 mA cm^{-2}, 0.43, and 1.62% for that based on PP-DBT:PCBM; and 0.76 V, 2.10 mA cm^{-2}, 0.40, and 0.65% for that based on PT-DBT: PCBM, respectively.

Comparing the device based on PT-DBT: PCBM, the V_{oc} of the device based on the PP-DBT: PCBM and PF-DBT: PCBM increases by ca. 0.20 and 0.28 V. Generally, V_{oc} is related to the difference between the HOMO energy level of donor (copolymer) and the LUMO energy level of acceptor (PCBM), so the higher V_{oc}s are consistent with the lower-lying HOMO energy levels of the PP-DBT (−5.23 eV) and PF-DBT (−5.45 eV).

As for the J_{sc}, the higher J_{sc} of the device based on PP-DBT: PCBM comparing with the device based on PF-DBT: PCBM could be explained by the broader absorption and lower bandgap of PP-DBT. However, it is strange that the device based on PT-DBT exhibits the lowest J_{sc} among the

Table 2. Optical and Electrochemical Properties of Copolymers

polymers	$\lambda_{max}^{abs,sol}$ (nm)	$\lambda_{max}^{abs,film}$ (nm)	E_g^{opt} (eV)	E_{ox}^{onset} (V)	HOMO (eV)	E_{red}^{onset} (V)	LUMO (eV)	E_g^{ec} (eV)
PF-DBT	400/436	400/449	2.32	0.71	−5.45	−1.69	−3.05	2.40
PP-DBT	462	474	2.24	0.50	−5.23	−1.75	−2.98	2.25
PT-DBT	485	505	2.02	0.38	−5.11	−1.72	−3.01	2.10

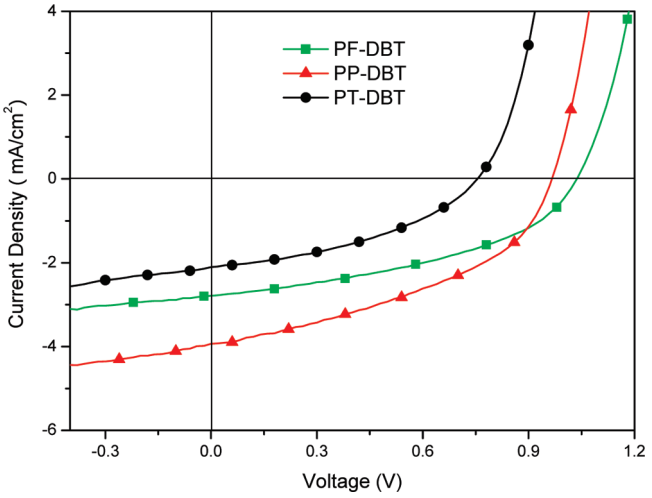

Figure 5. $J-V$ curves of the copolymer photovoltaic cells based on PF-DBT,PP-DBT and PT-DBT under the illumination of AM 1.5, 100 M_w/cm^2.

three devices though the absorbance of PT-DBT matches the solar radiation better than that of PF-DBT and PP-DBT, which could be due to the relatively low charge carrier mobility of PT-DBT, which was investigated in the following. Furthermore, the amount of the absorbed light depends not only on the edge of absorption wavelength but also on the intensity of the absorption. Comparing the absorption of PF-DBT, PP-DBT and PT-DBT in Figure 3, PT-DBT absorbs longer wavelength photons, which is beneficial to J_{sc}, but PP-DBT have higher absorption coefficients than PF-DBT and PT-DBT, and PF-DBT and PT-DBT have comparable absorption coefficients in solution and in film. That is one of the reasons why the device based on PP-DBT has a higher J_{sc} than the devices based on PF-DBT and PT-DBT.

As we know charge carrier mobility is very important to J_{sc}. To compare the three copolymers contributing the charge carrier mobility in the blend films, we measured the hole mobility of the three copolymers: PCBM blend films by space charge limited current (SCLC) method.[30] The hole-only devices with a structure of ITO/PEDOT/copolymer: PCBM/Au were fabricated. The hole mobilities were measured to be 8.2×10^{-6} cm^2 V^{-1} s^{-1}, 2.4×10^{-6} cm^2 V^{-1} s^{-1}, and $2.1\times10^{-7}cm^2$ V^{-1} s^{-1} for PF-DBT:PCBM, PP-DBT: PCBM, and PT-DBT:PCBM, respectively. Then the hole mobility of PT-DBT:PCBM is estimated to be about $2.1\times10^{-7}cm^2$ V^{-1} s^{-1}, about one order lower than that of PF-DBT:PCBM and PP-DBT:PCBM. That is why the J_{sc} of the cell based on PT-DBT:PCBM is lower than the cells based on PP-DBT:PCBM and PF-DBT:PCBM.

In bulk-heterojunction solar cells, the surface morphology of the active layer is very important to their photovoltaic performance.[36−38] Figure 6 shows the surface morphology of the active layers of PF-DBT:PCBM, PP-DBT:PCBM and PT-DBT:PCBM in AFM (atom force microscopy) images. Their surfaces are quite smooth. The root-mean-square (rms) roughness of the three active layers is 0.36, 0.88, and 0.63 nm, respectively. The PP-DBT:PCBM and PT-DBT: PCBM films have similar surface morphologies and rms roughness, while PF-DBT: PCBM has a different surface morphology and a lower rms. According to the bulk heterojunction solar cell model, the V_{oc} is determined by the energy difference between the HOMO level of the donor and the LUMO level of the acceptor,[14] and it is also influenced by the quality of the heterojunction, which is highly influenced by the film preparation conditions. But typically the changes in V_{oc} by the quality of the heterojunction are less than 0.1 V in reasonably prepared devices. In our case, the changes of V_{oc} for the three devices (1.05, 0.96, and 0.76 V) are significant. So we believe that although the morphologies are different for the three samples, and may play a role in the V_{oc} change, the main reason causing such a large change in V_{oc} is the HOMO level of the copolymer.

Table 3. Photovoltaic Properties of the Copolymer Photovoltaic Cells

1:4 wt ratio	V_{oc} (V)	J_{sc} (mA/cm^2)	FF (%)	PCE (%)
PF-DBT: PCBM	1.04	2.80	0.43	1.25
PP-DBT: PCBM	0.96	3.93	0.43	1.62
PT-DBT: PCBM	0.76	2.10	0.40	0.65

Figure 7 shows the input photon to current efficiency (IPCE) spectra of devices based on PF-DBT:PCBM, PP-DBT:PCBM, and PT-DBT:PCBM. The device based on PP-DBT shows the highest IPCE (the maximum IPCE of 40% at 435 nm) among the three devices, while the device based on PT-DBT exhibits the lowest IPCE in the visible spectral region due to the higher absorption coefficient of PP-DBT and the higher hole mobility of PP-DBT: PCBM blend film.

3. Conclusions

Novel 4,7-diphenyl-2,1,3-benzothiadiazole-based poly(heteroarylenevinylene)s were prepared by the Horner polycondensation route and characterized by NMR and elemental analysis. The polymers exhibit moderate to high molecular weights and are readily soluble in common organic solvents. The electrochemical properties indicated that these copolymers had relative low HOMO energy level and high air-stability, and the low HOMO energy level assured a relative high open circuit potential when they were used in photovoltaic cells. Photovoltaic cells preliminary results show that the PVCs based on PP-DBT delivered higher performance (1.62%) than those based on PF-DBT and PT-DBT, which should be ascribed to the relative broader absorption, lower band gap and higher hole mobility of PP-DBT.

4. Experimental Section

Materials. All starting materials were purchased from either Acros or Aldrich Chemical Co. and used without further purification, unless otherwise noted. In synthetic preparations, diethyl ether and THF were dried by distillation from sodium/ benzophenone under nitrogen. Similarly, DMF and dichloromethane were distilled from CaH_2 under nitrogen. 1,4-Dialkoxybenzene (**2**),[31] 1,4-dialkoxy-2,5-dibromobenzene (**3**),[32] 4-bromo-2,5-bis(dialkoxy)benzaldehyde (**4**),[33] 9,9-di-*n*-octylfluorene,[25] 4,7-dibromo-2,1,3-benzothiadiazole,[34] 1,4-bis(bromomethyl)-2-methoxy-5-(2-ethylhexyloxy)benzene (**8**),[16] and 3,4-dihexylthiophene[35] were prepared according to known literature procedures.

Measurement. ^1H NMR spectra were recorded on Bruker AVANCE 500-MHz spectrometer with chloroform-*d* as solvent and tetramethylsilane (TMS) as internal standard. The elemental analysis was carried out with a Thermoquest CHNS-Ovelemental

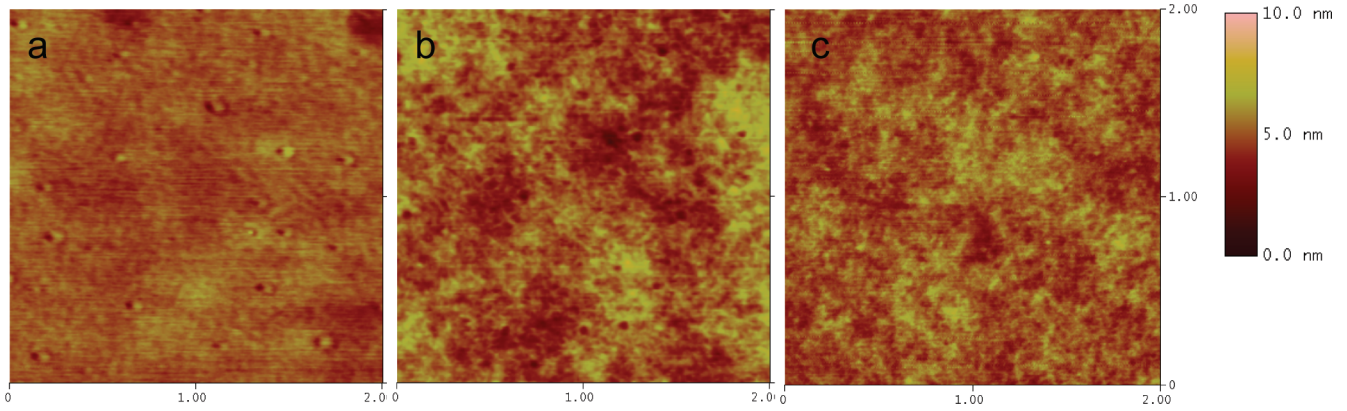

Figure 6. AFM images showing the morphology of the blend films spin-coated from chlorobenzene for copolymers: (a) height image of PF-DBT/PCBM (w/w, 1:4); (b) height image of PP-FBT/PCBM (w/w, 1:4); (c) height image of PT-DBT/PCBM (w/w, 1:4).

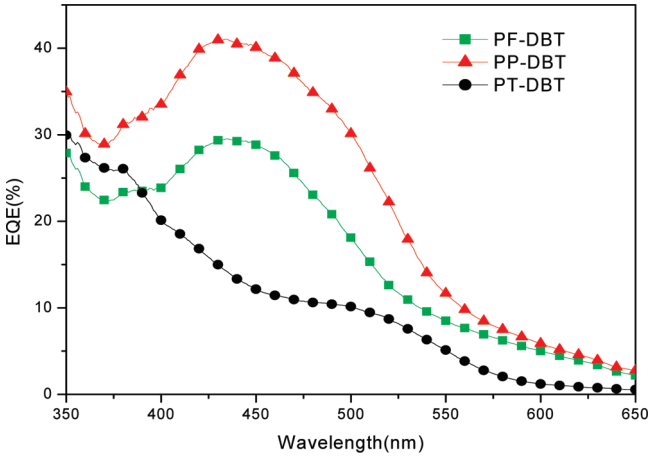

Figure 7. Input photon to current efficiency (IPCE) spectra of devices fabricated with copolymers/PCBM system.

analyzer. The gel permeation chromatographic (GPC) analysis was carried out with a Waters 410 instrument with tetrahydrofuran as the eluent (flow rate: 1 mL/min, at 35 °C) and polystyrene as the standard. The thermogravimetric analysis (TGA) was performed on a Perkine Elmer Pyris 1 analyzer under nitrogen atmosphere (100 mL/min) at a heating rate of 10 °C/min. UV−visible absorption spectra were measured using a Shimadzu UV-3100 spectrophotometer. Electrochemical measurements of these derivatives were performed with a Bioanalytical Systems BAS 100 B/W electrochemical workstation. Atomic force microscopy (AFM) images of blend films were carried out using a Nanoscope IIIa Dimension 3100.

Photovoltaic Device Fabrication and Characterization. The polymer PVCs were fabricated with the active layer consisting of the copolymers (PF-DBT, PP-DBT and PT-DBT): PCBM in 1:4 wt/wt ratio, respectively. The ITO glass substrates were precleaned by detergent, acetone and boiled in H_2O_2. Highly conducting poly(3,4-ethylenedioxythiophene):poly(sty-enesulfonate) (PEDOT:PSS, Baytron P, Al4083) was spin-casted (3000 rpm) in a thickness of ∼ 40 nm from aqueous solution (after passing through a 0.45 μm filter). The substrate was annealed at 120 °C for 15 min on hot plate. The copolymers were dissolved in chlorobenzene to make 5 mg mL^{-1} solutions, followed by blending with PCBM (purchased from Lumtec. Corp) in 80 wt %. The active layers were obtained by spin-coating the blend solutions at 1000 rpm for 30 s and the thickness of films were ∼ 90 nm, as measured with the Ambios Technology XP-2. Subsequently, LiF (0.6 nm) and Al (100 nm) electrodes were deposited via thermal evaporation in vacuum (5×10^{-4} Pa) in thickness of approximately. The hole-only devices with a general structure of ITO/PEDOT:PSS/copolymer:PCBM(90 nm)/Au (60 nm) were fabricated for hole mobility measurement by space-charge-limited current (SCLC) method. The active area was about 5 mm^2. Current−voltage *(J-V)* characteristics were recorded using Keithley 2400 Source Meter in the dark and under 100 mW/cm^2 simulated AM 1.5 G irradiation (Sciencetech SS-0.5K Solar Simulator). All the measurements were performed under ambient atmosphere at room temperature.

2-(4-Bromo-2,5-bis(hexyloxy)phenyl)-[1,3]dioxane (5). To a solution of 4-bromo-2,5-bis(dialkoxy)benzaldehyde (**4**) (8.0 g, 20.78 mmol) and propane-1,3-diol (1.75 g, 22.86 mmol) in toluene (30 mL) was added $BF_3 \cdot OEt_2$ (3−4 drops). This mixture was refluxed for 8 h in a Dean−Stark apparatus to remove the theoretical amount of water. The solution was washed with 1 M aqueous $NaHCO_3$ and then with water, dried over $MgSO_4$, and concentrated in a vacuum to give **5** (7.02 g, 87%) as a brown liquid, which was sufficiently pure to be employed in the next step.

4-Formyl-2,5-bis(hexyloxy)phenylboronic Acid (6). A 2.5 M solution of *n*-butyllithium (5.54 mL, 13.84 mmol) was added to a nitrogen-purged solution of 2-(4-bromo-2,5-bis(hexyloxy)phenyl)[1,3]dioxane (**5**) (5.57 g, 12.60 mmol) in anhydrous THF (30 mL) at −78 °C using a syringe. The solution was then stirred for 2 h. Trimethyl borate (1.57 g, 15.11 mmol) was added with a syringe. The resulting mixture was allowed to come to room temperature and stir for 24 h. Then it was cooled to 0 °C, 2 M HCl (25 mL) was added, and the mixture was held at room temperature for an additional 20 h. The organic layer was separated and the aqueous layer was extracted with diethyl ether (3×100 mL). The combined ether layers were washed twice with 100 mL of water and brine and dried over $MgSO_4$. After filtration, solvent was then removed under reduced pressure. The crude product was purified by recrystallization from hexane to give a light yellow powder. Yield: 3.43 g (78%).

^{1}H NMR (500 MHz, $CDCl_3$): δ 10.50 (s, 1H), 7.50 (s, 1H), 7.31 (s, 1H), 6.10 (br, 2H), 4.10 (t, $J = 6.0$ Hz, 2H), 4.07 (t, $J =$ 6.5 Hz, 2H), 1.86−1.79 (m, 4H), 1.50−1.42 (m, 4H), 1.37−1.33 (m, 8H), 0.92−0.87 (m, 6H). Anal. Calcd for $C_{19}H_{31}BO_5$: C, 65.15; H, 8.92. Found: C, 65.02; H, 9.08.

4,4′-(2,1,3-benzothiadiazole-4,7-diyl)bis(2,5-bis(hexyloxy) benzaldehyde) (M-1). Under a nitrogen atmosphere, 4,7-Dibromo-2,1,3-benzothiadiazole (0.88 g, 3.0 mmol) and 4-formyl-2,5-bis(hexyloxy) phenylboronic acid (2.53 g, 7.22 mmol) were added to degassed aqueous solution of potassium carbonate 10 mL (2.0 M), toluene, and THF 40 mL (1:1, volume ratio). After 30 min of degassing, 3 mol % (104 mg, 0.09 mmol) of Pd-$(PPh_3)_4$ was added. The mixture was stirred vigorously at 85 °C for 36 h under a nitrogen atmosphere. The reaction mixture was cooled to room temperature, followed by the addition of toluene and water. The organic layer was separated and washed with

water and brine and dried over $MgSO_4$. After filtration, solvent was then removed under reduced pressure. The crude product was purified by silica gel column chromatography (hexane/ethyl acetate = 20:1) to give a light yellow powder. Yield: 1.30 g (58%).

^{1}H NMR (500 MHz, $CDCl_3$): δ 10.55 (s, 2H), 7.82 (s, 2H), 7.52 (s, 2H), 7.31 (s, 2H), 4.09 (t, J = 6.5 Hz, 4H), 4.00 (t, J = 6.5 Hz, 4H), 1.88−1.82 (m, 4H), 1.60−1.54 (m, 4H), 1.52−1.46 (m, 4H), 1.38−1.32 (m, 8H), 1.23−1.14 (m, 12H), 0.91 (t, J = 7.0 Hz, 6H), 0.80 (t, J = 7.0 Hz, 6H). ^{13}C NMR (75 MHz, $CDCl_3$): 189.38, 155.81, 153.80, 150.67, 134.03, 130.32, 129.84, 125.00, 116.94, 110.66, 69.29, 69.15, 31.52, 31.31, 29.18, 28.95, 25.74, 25.55, 22.58, 22.51, 14.01, 13.93. Anal. Calcd for $C_{44}H_{60}N_2O_6S$: C, 70.93; H, 8.12; N, 3.76, S, 4.30. Found: C, 70.68; H, 8.23; N, 3.68 ; S, 4.26.

2,7-Bis(bromomethyl)-9,9-di-*n*-octylfluorene (7). A mixture of 2.0 g (5.12 mmol) of 9,9-Di-n-octylfluorene, 0.9 g (30 mmol) of paraformaldehyde, and 15 mL of 33% concentrated hydrogen bromide in acetic acid was stirred at 70 °C for 24 h. After cooling to room temperature, the reaction mixture was slowly poured into saturated $NaHCO_3$ solution, extracted with CH_2Cl_2, and washed with water and brine. The combined extract was dried over Na_2SO_4. After removal of the solvent, the crude product was purified by column chromatography using petroleum ether as an eluent to obtain **7** in 67% yield.

^{1}H NMR (500 MHz $CDCl_3$): δ 7.63 (d, J = 7.5 Hz, 2H,), 7.38−7.32 (m, 4H), 4.60 (s, 4H, $-CH_2$Br), 1.94(m, 4H), 1.22−1.01 (m, 20H), 0.81 (t, J = 7.0 Hz, 6H), 0.65−0.55 (m, 4H).

2,7-Bis(methylenediethyl phosphate)-9,9-di-*n*-octylfluorene (M-2). A strirred mixture of compound **7** (2.02 g, 3.5 mmol) and triethyl phosphite (4.0 mL, 24 mmol), under nitrogen was heated at 150 °C for 24 h. Excess triethyl phosphite was removed by vacuum distillation. The crude product was purified by column chromatography (AcOEt/MeOH, 95:5) to give 82% of monomer (**M-2**) as yellowy liquid.

^{1}H NMR (500 MHz $CDCl_3$): δ 7.60 (d, J = 8.0 Hz, 2H,), 7.26−7.24 (m, 4H,), 4.04−3.95 (m, 8H, OCH_2CH_3), 3.23 (d, J = 21.5 Hz, CH_2P), 1.94 (m, 4H), 1.23 (t, J = 7.0 Hz, 12H, OCH_2CH_3), 0.96−1.2 (m, 20H,), 0.81 (t, J = 7.0 Hz, 6H), 0.56−0.53 (m, 4H). ^{13}C NMR (75 MHz $CDCl_3$): 150.84, 139.51, 130.16, 130.03, 128.40, 128.31, 124.09, 124.00, 119.52, 62.03, 61.94, 54.81, 40.37, 34.86, 33.04, 31.65, 30.01, 29.28, 29.16, 23.75, 22.43, 16.30, 13.94.

2-Methoxy-5-(2-ethylhexyloxy)-1,4-xylylenebis(diethylphosphonate) (M-3). Compound **8** (4.22 g, 10.0 mmol) reacted with triethyl phosphite (10.3 mL, 60.0 mmol) at 150 °C for 24 h. Excess triethyl phosphite was removed by vacuum distillation. The crude product was purified by column chromatography (AcOEt/ Hexane, 1:2) to give 87% of monomer (**M-3**) as white solid.

^{1}H NMR (500 MHz, $CDCl_3$): 6.97 (S, 1H), 6.91(S,1H), 4.10−4.00 (m, 8H, OCH_2CH_3), 3.85−3.80 (m, 5H), 3.28−3.19 (m, 4H, CH_2P), 1.75−1.68 (m, 1H), 1.55−1.37 (m, 4H), 1.35−1.30 (m, 4H), 1.28−1.21 (m, 12H, OCH_2CH_3), 0.96−0.89 (m, 6H). ^{13}C NMR (75 MHz $CDCl_3$): 150.35, 118.99, 114.44, 113.57, 70.77, 61.50, 55.76, 39.31, 30.25, 28.76, 26.38, 25.05, 23.57, 22.69, 16.00, 13.71, 10.81.

2,5-Bis(bromomethyl)-3,4-dihexylthiophene (9). A two necked flask containing 5.0 g (19.8 mmol) of 3,4-dihexylthiophene, and 3.6 g (120 mmol) of paraformaldehyde was placed in an ice bath. To this flask, 30 mL of 33% HBr solution in acetic acid was added carefully, and the mixture was stirred for 24 h at 70 °C. The reaction was diluted with 200 mL of ethyl ether and washed with water, saturated $NaHCO_3$ solution, and brine. After the solvent removal, 6.06 g of light brown oil was obtained (70% yield), which was sufficiently pure for next step reaction.

3,4-Dihexyl-2,5-bis(methylenediethyl phosphate)thiophene (M-4). Compound **9** (4.38 g, 10.0 mmol) reacted with triethyl phosphite (10.5 mL, 61.2 mmol) at 150 °C for 24 h. The crude product was purified by column chromatography on silica gel using acetone-hexane (25:75) as an eluent to give 4.20 g of light yellow oil (76% yield).

^{1}H NMR (500 MHz, $CDCl_3$): δ 4.11−4.05 (m, 8H, OCH_2CH_3), 3.30−3.24 (m, 4H, CH_2P), 2.49 (t, J = 7.5 Hz, 4H), 1.48−1.29 (m, 28H), 0.92 (t, J = 7.0 Hz, 6H). ^{13}C NMR (75 MHz, $CDCl_3$): 139.96, 124.53, 62.25, 31.63, 30.58, 29.53, 27.48, 27.23, 25.55, 22.59, 16.34, 14.02.

Polymer Synthesis. *General Procedure for Horner−Wadsworth−Emmons Polycondensation Poly(fluorenevinylene-alt-4,7-diphenyl-2,1,3-benzothiadiazole) (PF-DBT).* The dicarboxyaldehyde (**M-1**) (0.30 g, 0.40 mmol) and monomer (**M-2**) (0.28 g, 0.40 mmol) were dissolved in 20 mL of anhydrous THF under nitrogen. To this solution was added potassium tertbutoxide (2 mL of a 1 M solution in THF). The reaction was stirred for 40 h at room temperature under nitrogen. The polymer was precipitated into 400 mL of methanol and filtered through a Soxhlet thimble, which was then subjected to Soxhlet extraction with methanol, hexane, acetone, and chloroform. The fraction from chloroform was concentrated under reduced pressure and precipitated into methanol (300 mL), collected by filtration. The final product was dried under vacuum overnight to afford **PF-DBT** as an orange yellow solid (0.31 g, 68%).

^{1}H NMR (500 MHz, $CDCl_3$): 7.84 (br, 2H), 7.71(d, J = 7.5 Hz, 2H,) 7.66−7.55(m, 4H), 7.37−7.26 (m, 8H, aromatic and vinylic), 4.12−4.00 (m, 8H), 2.04 (br, 4H), 1.92 (t, J = 6.5, 4H), 1.59 (br, 8H), 1.42 (br, 8H), 1.30−1.03 (m, 32H), 0.95 (t, J = 6.5, 6H), 0.83 (t, J = 7.5, 12H), 0.76−0.55 (m, 4H). ^{13}C NMR (125 MHz, $CDCl_3$): 154.73, 151.98, 151.34, 141.07, 137.32, 130.88, 130.26, 128.19, 127.28, 126.00, 123.22, 121.48, 120.28, 117.39, 117.09, 69.99, 55.40, 32.21, 32.09, 31.84, 30.57, 30.12, 29.87, 29.71, 26.42, 26.09, 24.27, 22.99, 14.49, 14.41. Anal. Calcd for $(C_{75}H_{102}N_2O_4S)_n$: C, 79.68; H, 9.12; N, 2.48; S, 2.84. Found: C, 78.52; H, 8.93; N, 2.25 ; S, 2.36.

Similarly, the monomers **M-3** and **M-4** and dicarboxyaldehyde (**M-1**) were polymerized using potassium *tert*-butoxide to obtain the polymers poly(phenylenevinylene-*alt*-4,7-diphenyl-2,1,3-benzothiadiazole) (**PP-DBT**), poly(thiophenevinylene-*alt*-4,7-diphenyloxadiazole) (**PT-DBT**). The yield and molecular weights of the polymers are summarized in Table 1.

PP-DBT. Yield = 70%. ^{1}H NMR (500 MHz, $CDCl_3$): 7.82 (br, 2H), 7.65−7.54 (m, 4H), 7.43−7.23 (m, 6H, aromatic and vinylic), 4.15−3.88 (m, 13H, $-OCH_2-$ and $-OCH_3$), 1.89(br, 5H),1.67−1.50 (m, 12H), 1.38 (br, 12H), 1.22 (br, 12H), 1.03−0.89 (m, 12H), 0.83 (br, 6H). Anal. Calcd for $(C_{61}H_{84}N_2O_6S)_n$: C, 75.27; H, 8.70; N, 2.88; S, 3.29. Found: C, 74.85; H, 9.24; N, 2.53 ; S, 3.01.

PT-DBT. Yield = 65%. ^{1}H NMR (500 MHz, $CDCl_3$): 7.81 (br, 2H), 7.54−7.49(m, 2H), 7.26−7.19(m, 6H, aromatic and vinylic), 4.10−3.97 (m, 8H), 2.66 (br, 4H), 1.95−1.87 (m, 4H), 1.58 (br, 12H), 1.43−1.32 (m, 18H), 1.20 (br, 12H), 0.96−0.89 (m, 12H), 0.85−0.80 (m, 6H). ^{13}C NMR (75 MHz, $CDCl_3$): 154.21, 150.86, 150.63, 141.56, 136.09, 130.38, 129.70, 127.57, 126.42, 123.37, 122.25, 116.23, 112.41, 69.53, 69.29, 31.70, 31.60, 31.37, 29.54, 29.41, 29.20, 25.83, 25.60, 22.65, 22.52, 14.09, 13.98. Anal. Calcd for $(C_{62}H_{88}N_2O_4S_2)_n$: C, 75.26; H, 8.96; N, 2.83; S, 6.48. Found: C, 74.30; H, 8.40; N, 2.48 ; S, 6.09.

Acknowledgment. This work was supported by the State Key Development Program for Basic Research of China (Grant No.2009CB623605), the National Natural Science Foundation of China (Grant No. 50673035, 20874035), Program for New Century Excellent Talents in Universities of China Ministry of Education, the 111 Project (Grant No. B06009), and the Project of Jilin Province (20080305). The authors thank Dr. Wenchao Dou and Dr. Songnan Qu for helpful suggestions.

References and Notes

(1) Leclerc, N.; Michaud, A.; Sirois, K.; Morin, J.-F.; Leclerc, M. *Adv. Funct. Mater*. **2006**, *16*, 1694–1704.

(2) Zhang, F. L.; Mammo, W.; Andersson, L. M.; Admassie, S.; Andersson, M. R.; Inganäs, O. *Adv. Mater.* **2006**, *18*, 2169–2173.
(3) Zhu, Z. G.; Waller, D.; Gaudiana, R.; Morana, M.; Mulhlbacher, D.; Scharber, M.; Brabec, C. *Macromolecules* **2007**, *40*, 1981–1986.
(4) Hou, J. H.; Park, M.-H.; Zhang, S. Q; Yao, Y.; Chen, L. M.; Li, J.-H.; Yang, Y. *Macromolecules* **2008**, *41*, 6012–6018.
(5) Blouim, N.; Michaud, A.; Gendron, D.; Wakim, S.; Blair, E.; Neagu-Plesu, R.; Durocher, G.; Tao, Y.; Leclerc, M. *J. Am. Chem. Soc.* **2008**, *130*, 732–742.
(6) Geng, J. L.; Zeng, T. Y. *J. Am. Chem. Soc.* **2006**, *128*, 16827–16833.
(7) Blom, P. W. M.; Mihailetchi, V. D.; Koster, L. J. A.; Markov, D. E. *Adv. Mater.* **2007**, *19*, 1551–1566.
(8) Li, G.; Shrotriya, V.; Huang, J. S.; Yao, Y.; Moriarty, T.; Emery, K.; Yang, Y. *Nat. Mater.* **2005**, *4*, 864–868.
(9) Ma, W. L.; Yang, C. Y.; Gong, X.; Lee, K. H.; Heeger, A. J. *Adv. Funct. Mater.* **2005**, *15*, 1617–1622.
(10) Yip, H.-L.; Hau, S. K.; Baek, N. S.; Ma, H.; Gen, A. K-Y. *Adv. Mater.* **2008**, *20*, 2376–2382.
(11) Li, G.; Shrotriya, V.; Huang, J.; Yao, Y.; Moriarty, T.; Emery, K.; Yang, Y. *Nat. Mater.* **2005**, *4*, 864–868.
(12) Chen, C.-P.; Chan, S.-H.; Chao, T-Ch.; Ting, C.; Ko, B.-T. *J. Am. Chem. Soc.* **2008**, *130*, 12828–12833.
(13) Xiao, S. Q.; Zhou, H. X.; You, W. *Macromolecules* **2008**, *41*, 5688–5696.
(14) Scharher, M. C.; Mühlbacher, D.; Koppe, M.; Denk, P.; Waldauf, C.; Heeger, A. J.; Brabec, C. *J. Adv. Mater.* **2006**, *18*, 789–794.
(15) Wen, S. P.; Pei, J. N.; Zhou, Y. H.; Xue, L. L.; Xu, B.; Li, Y. W.; Tian, W. J. *J. Polym. Sci., Part A: Polym. Chem.* **2009**, *47*, 1003–1012.
(16) Hou, J. H.; Park, M.-H.; Zhang, S. Q; Yao, Y.; Chen, L. M.; Li, J.-H.; Yang, Y. *Macromolecules* **2008**, *41*, 6012–6018.
(17) Liu, J.; Bu, L. J.; Dong, J. P.; Zhou, Q. G.; Geng, Y. H.; Ma, D. G.; Wang, L. X.; Jing, X. B.; Wang, F. S. *J. Mater. Chem.* **2007**, *17*, 2832–2838.
(18) Zhang, X. L.; Gorohmaru, H.; Kadowaki, M.; Kobayashi, T.; Ishi-I, T.; Thiemann, T.; Mataka, S. *J. Mater. Chem.* **2004**, *14*, 1901–1904.
(19) Kato, S. I.; Matsumoto, T.; Shigeiwa, M.; Gorohmaru, H.; Maeda, S.; Ishi-i, T.; Shuntaro Mataka, M. *Chem.—Eur. J.* **2006**, *12*, 2303–2317.
(20) Thomas, J. K. R.; Lin, J. T.; Velusamy, M.; Tao, Y.-T.; Chuen, C.-H. *Adv. Funct. Mater.* **2004**, *14*, 83–90.
(21) Fu, Y. P.; Cheng, H. T.; Elsenbaumer, R. L. *Chem. Mater.* **1997**, *9*, 1720–1724.
(22) Egbe, D. A. M.; Tillmann, H.; Birckner, E.; Klemm, E. *Macromol. Chem. Phys.* **2001**, *202*, 2712.
(23) Shahid, M.; Ashraf, R. S.; Klemm, E.; Sensfuss, S. *Macromolecules* **2006**, *39*, 7844–7853.
(24) Amrutha, S. R.; Jayakannan, M. *J. Phys. Chem. B.* **2006**, *110*, 4083–4091.
(25) Anuragudom, P.; Newaz, S. S.; Phanichphant, S.; Lee, T. R. *Macromolecules* **2006**, *39*, 3494–3499.
(26) Yamamoto, T.; Komarudin, D.; Arai, M.; Lee, B. L.; Suganuma, H.; Asakawa, N.; Inoue, Y.; Kubota, K.; Sasaki, S.; Fukuda, T.; Matsuda, H. *J. Am. Chem. Soc.* **1998**, *120*, 2047–2058.
(27) Peng, Q.; Park, K.; Lin, T.; Durstock, M.; Dai, L. M. *J. Phys. Chem. B.* **2008**, *112*, 2801–2808.
(28) Hou, J. H.; Tan, Z. A.; Yan, Y.; He, Y. J.; Yang, C. H.; Li, Y. F. *J. Am. Chem. Soc.* **2006**, *128*, 4911–4916.
(29) Shi, C. J.; Yao, Y.; Yang, Y.; Pei, Q. B. *J. Am. Chem. Soc.* **2006**, *128*, 8980–8986.
(30) Blom, P. W. M.; deJong, M. J. M.; vanMunster, M. G. *Phys. Rev. B* **1997**, *55*, R656–R659.
(31) Egbe, D. A. M.; Tillmann, H.; Birckner, E.; Klemm, E. *Macromol. Chem. Phys.* **2001**, *202*, 2712–2726.
(32) Maruyama, S.; Kawanishi, Y. *J. Mater. Chem.* **2002**, *12*, 2245–2249.
(33) Wright, M. E.; Mullick, S.; Lackritz, H. S.; Liu, L. Y. *Macromolecules* **1994**, *11*, 3009–3015.
(34) Pilgram, K.; Zupan, M.; Skile, R. *J. Heterocycl. Chem.* **1970**, *7*, 629–633.
(35) Ashraf, R. S.; Klemm, E. *J. Polym. Sci., Part A: Polym. Chem.* **2005**, *43*, 6445–6454.
(36) Liu, J.; Shi, Y. J.; Yang, Y. *Adv. Funct. Mater.* **2001**, *11*, 420–424.
(37) Zhou, Y. H.; Wang, Y. N.; Wu, W, C.; Wang, H.; Han, L.; Tian, W. J.; Bassler, H. *Sol. Energy Mater. Sol. Cells* **2007**, *91*, 1842–1848.
(38) Shaheen, S. E.; Brabec, C. J.; Sariciftci, N. S.; Padinger, F.; Fromherz, T.; Hummelen, J. C. *Appl. Phys. Lett.* **2001**, *78*, 841–843.